today or the austral sink radically enhanced, starting at the time of the boreal methane rise and fortuitously stopping at the time of the austral methane rise. Thus, we argue that the Boreal burst scenario is extremely unlikely.

44. S. Frolking and P. Crill, *Global Biogeochem. Cycles* **8**, 385 (1994).
45. W. S. Broecker and G. H. Denton, *Geochim. Cosmochim. Acta* **53**, 2465 (1989); S. Manabe and R. J. Stouffer, *Nature* **378**, 165 (1995); S. Rahmstorf, *Nature* **378**, 145 (1995).
46. A. M. Ágústsdóttir, R. B. Alley, D. Pollard, W. H. Peterson, *Geophys. Res. Lett.* **26**, 1333 (1999).
47. P. A. Mayewski *et al.*, *Science* **263**, 1747 (1994).
48. S. W. Hostetler, P. U. Clark, P. J. Bartlein, A. C. Mix, N. J. Pisias, *J. Geophys. Res.* **104**, 3947 (1999). We speculate that abrupt warming in the North Atlantic basin may have stimulated the Asian monsoon by the decrease in continental albedo associated with reduced snow cover and greening of desert in downwind Eurasia.

49. $\delta^{18}O_{ice}$ was converted to temperature for the purpose of forcing the nitrogen and argon isotope model by means of the relation T (degrees Celsius) = ($\delta^{18}O_{ice}$ − 1.3 per mil)/(0.384 per mil K^{-1}) + 60. The 1.3 per mil was subtracted from glacial $\delta^{18}O_{ice}$ to account for the glacial seawater $\delta^{18}O$ change due to ice volume. The coefficient 0.384 and constant of 60 were obtained by forcing the equation to predict a temperature of −47.5°C during the Oldest Dryas (*51*) and a mean for the last 1000 years of −31°C from respective $\delta^{18}O_{ice}$ values of −40 per mil and −35.04 per mil (*5*). The firn heat and gas model consists of a separate firn heat model adapted from (*52*) that drives a firn gas diffusion model. The gas model is based on the diffusion equation, modified to include gravitational settling and thermal diffusion:

$$\frac{\partial C}{\partial t} = \frac{\partial}{\partial z}\left\{ D(z,T)\left[\frac{\partial C}{\partial z} - \frac{\Delta m g}{RT} + \Omega\frac{dT}{dz}\right]\right\}$$

where C is isotope delta value (for example, $\delta^{15}N$), t is time, D is molecular diffusivity of gas in porous snow, and the other symbols are as defined in the text. The model is discretized on a 5-m grid, with a time step of 8 days, with diffusivities calculated from an empirical diffusivity-density relation based on observed CO_2 concentrations in South Pole firn air after (*50*). The density profile was modeled from (*53*). To assign gas ages, we assumed a mean gas age at the time of bubble closure of 15 years. The heat model was forced at the top boundary condition (that is, the surface) with temperature calculated from $\delta^{18}O_{ice}$. The bottom boundary of the heat model was held at 1000 m to account for the thermal inertia of the ice. The bottom boundary of the gas model is impermeable and held constant at 95-m depth, the firn depth inferred from the Herron-Langway model (*53*) with an accumulation rate of 0.07 m of ice per year and a temperature of −47.5°C (*51*).

50. M. Battle *et al.*, *Nature* **383**, 231 (1996).
51. K. Cuffey and G. Clow, *J. Geophys. Res.* **102**, 26383 (1997).
52. R. B. Alley and B. R. Koci, *Ann. Glaciol.* **14**, 6 (1990).
53. M. M. Herron and C. C. Langway, *J. Glaciol.* **25**, 373 (1980).
54. M. Bender *et al.*, *Nature* **372**, 663 (1994).

55. We thank M. Bender for helpful discussions and for hosting us in his laboratory at the University of Rhode Island, where many of these measurements were made; J. Orchardo for technical assistance; T. Ellis for the firn air $\delta^{15}N$ analyses; B. Luz for developing the $^{40}Ar/^{36}Ar$ technique for air samples; L. Tuttle and S. Cowburn for methane measurements at Washington State University; A. Grachev for the thermal diffusion sensitivity measurements; D. Mastroianni for the $\delta^{15}N$ measurements at SIO; and R. Alley, T. Sowers, R. Keeling, D. Jacob, L. Talley, and S. Harder for helpful discussions. This work was supported by NSF grants OPP 9725305 (J.P.S.) and OPP 9725918 (E.J.B.).

11 June 1999; accepted 1 October 1999

REPORTS

16°C Rapid Temperature Variation in Central Greenland 70,000 Years Ago

C. Lang,[1]* M. Leuenberger,[1]* J. Schwander,[1] S. Johnsen[2,3]

Variations in the $^{29}N_2/^{28}N_2$ ratio of air bubbles trapped in polar ice cores and their relation to variations of the $^{18}O/^{16}O$ of the ice allow past surface temperature variations and ice age–gas age differences to be determined. High-resolution measurements of $^{29}N_2/^{28}N_2$ in Dansgaard-Oeschger event 19 (around 70,000 years before the present) in ice from Central Greenland show that at the beginning of the event, the ice age–gas age difference was 1090 ± 100 years. With the use of a combined firn densification, temperature, and gas diffusion model, the $\delta^{18}O_{ice}$-temperature coefficient α was determined to be 0.42 ± 0.05 per mil per kelvin. This coefficient implies a mean surface temperature change of 16.0 kelvin (between 14.3 and 18.1 kelvin), which differs substantially from values derived from borehole temperatures and modern spatial $\delta^{18}O_{ice}$–surface temperature correlations.

Dansgaard-Oeschger (DO) events are characterized by rapid increases in the stable oxygen isotope composition of the ice [$\delta^{18}O_{ice}$ (*1*)] in ice cores of the last glacial period to high values that persist for several hundred to several thousand years. When these increases were discovered [in Camp Century ice (*2*)], it was not clear whether they reflected drastic changes in Arctic (or even Northern Hemispheric) climate, local effects, or stratigraphic disturbances in the core. Their climatic relevance was shown by their widespread geographic extent (*3*), and they are now interpreted as warmer interstadial periods. Several attempts have been made to estimate these temperature variations, with the contemporary surface temperature–$\delta^{18}O_{ice}$ correlation, borehole temperature measurements, and differences between gas age and ice age (Δage) based on $\delta^{18}O_{ice}$-methane and $\delta^{15}N$-$\delta^{18}O_{ice}$ correlations. The correlation of modern mean annual surface temperature and the mean $\delta^{18}O_{ice}$ of precipitation at various sites in Greenland (spatial correlation) leads to a coefficient, α (= $\Delta\delta^{18}O_{ice}/\Delta T$, where T is temperature), of 0.67 per mil/K (*4*). Deconvolutions of borehole temperatures show that α may vary over climatic cycles, with similar values during the Holocene (α = 0.53 to 0.67 per mil/K) and different values for the last glacial termination (α = 0.3 to 0.33 per mil/K) (*5*, *6*), although no analogous conclusions can be drawn for the relatively short DO events. Studying the GRIP (Greenland Ice Core Project) and GISP2 (Greenland Ice Sheet Project 2) methane and $\delta^{18}O_{ice}$ records, Schwander *et al.* suggested (on the basis of the calculated Δages) an α of 0.4 to 0.5 per mil/K for the DO events between 40,000 and 20,000 years before the present (yr B.P.) (*7*). Using the same approach with nitrogen isotope ratios, Severinghaus *et al.* (*8*) obtained a value of about 0.30 per mil/K for the transition at the end of the Younger Dryas cold period, in agreement with the borehole temperature studies.

Here we present a reconstruction of the surface temperature change in Central Greenland during DO 19 (70,000 yr BP), based on high-resolution measurements of nitrogen isotopes on the GRIP ice core. This reconstruction provides us with an estimate of the relation between temperature and $\delta^{18}O_{ice}$ for a DO event. We chose DO 19 because it is one of the larger events during the glacial, with a $\delta^{18}O_{ice}$ change of +6.7 per mil (uncertainty of 0.05 per mil). If the present-day spatial relation (α = 0.67 per mil/K) is applied to the $\delta^{18}O_{ice}$ change, a temperature shift of 10°C is expected. With the glacial-Holocene borehole sensitivity (0.3 to 0.33 per mil/K), this $\delta^{18}O_{ice}$ change would correspond to a far larger 20° to 22°C temperature shift.

Because the isotope ratio of atmospheric nitrogen ($\delta^{15}N$) is constant over several hundred thousand years (*9*), changes of this ratio in the air trapped in the ice reflect processes that occur in the firn. These are gravitational enrichment of the heavier molecules at the bottom of the firn column, which is proportional to the height of the diffusive firn column (*10*, *11*), and thermal diffusion effects due to temperature gradients between the surface and the bottom of the firn column, which force the heavier molecules generally to migrate toward the colder end of the firn column. The fractional deviation of $\delta^{15}N$ due to thermal diffusion in equilibrium is given by (*12*)

[1]Climate and Environmental Physics, Physics Institute, University of Bern, Sidlerstrasse 5, Bern CH-3012, Switzerland. [2]Niels Bohr Institute, Department of Geophysics, University of Copenhagen, Juliane Maries Vej 30, DK-2100 Copenhagen, Denmark. [3]Science Institute, University of Iceland, Dunhaga 3, IS-107 Reykjavik, Iceland.

*To whom correspondence should be addressed. E-mail: lang@climate.unibe.ch (C.L.) or leuenberger@climate.unibe.ch (M.L.)

$$\Delta\delta^{15}N_{therm} = \left(\frac{R}{R_0} - 1\right) \times 1000 \text{ per mil}$$

$$= \left[\left(\frac{T_s}{T_b}\right)^{\alpha_T} - 1\right] \times 1000 \text{ per mil}$$

$$\cong \alpha_T\left(\frac{\Delta T}{T_b}\right) \times 1000 \text{ per mil}$$

where ΔT is the temperature difference between the bottom (T_b) and the surface (T_s) of the diffusive firn column, R is the isotope ratio compared with a reference (atmospheric) ratio R_0, and α_T is the thermal diffusion factor of $^{15}N^{14}N/^{14}N_2$. We used a temperature-dependent thermal diffusion factor of $\alpha_T = 4.61198 \times 10^{-3} \times \ln(T/113.65\ K)$ with a very small uncertainty of less than 0.1% (*13*, *14*). This thermal diffusion effect enables us to quantify past temperature changes if the response of the bottom temperature to surface temperature changes is calculated.

The air trapped in bubbles in ice is younger than the surrounding ice, because of the diffusion of the air through the porous firn to the ice below, where bubbles are formed. This difference between the age of the ice and the mean age of the gas, Δage, depends mainly on the advection velocity of the ice (which is a function of accumulation rate) and the depth of the firn column (which varies with temperature and accumulation rate) but less on the diffusivity of the considered gas species.

A plot of $\delta^{15}N$ (*15*) versus ice age for the GRIP ice core (*6*) (Fig. 1) reveals that at about 71,000 years B.P., $\delta^{15}N$ increases sharply by 0.17 ± 0.02 per mil in 160 years and then decreases slowly. The maximum change in $\delta^{15}N$, assuming no change in the diffusive column height but corrected for modeled gravitational fractionation, is equivalent to a temperature difference in the firn of 10.4 ± 1.6 K. The Δage is well represented by the shift between the $\delta^{15}N$ and $\delta^{18}O_{ice}$ curves. Because both records reflect variations in the surface temperature [assuming a correlation between surface and cloud temperatures as has been shown for Antarctica (*16*)], the age difference between gas and ice can be calculated by matching the ice ages of the corresponding points of the two signals. By comparing the two midpoints of the increases, we obtained an age difference of 1090 ± 100 years at the start of the event, whereas it is substantially lower during the DO 19 event (see model calculations in Fig. 1). The difference in depth between ice and gas signal is 4.20 ± 0.08 m. As layer counting at this depth is not possible or at least highly tentative, we used the GRIP SS09 age scale (*17*) with an approximate absolute uncertainty of 7% at 70,000 years B.P. The Δage, however, does not depend strongly on the absolute time scale but more on the relative timing, which is mainly dependent on the accumulation rate. A sensitivity study performed with our model showed that increasing or decreasing the accumulation rate by 10% results in an opposite 8% change in the Δage.

The coefficient that relates the oxygen isotopic composition of water and surface temperature ($\alpha = \Delta\delta^{18}O_{ice}/\Delta T_s$) can be derived in two ways from nitrogen isotope data. First, it can be calculated from the magnitude of the $\delta^{15}N$ change itself (*13*). Because this change reflects the temperature difference between the surface and the close-off depth, the heat diffusion through the ice must be calculated. Additionally, the gravitational fractionation needs to be considered, but that is of minor influence in the case of rapid temperature variations. Second, Δage can be used to derive α because Δage is a function of densification and air diffusion processes in the firn, which depend on accumulation rate and (less) on temperature (*8*). Calculations for both methods were performed with the same combined temperature/gas diffusion and firn densification model (*7*) for several α scenarios, that is, different temperature inputs. Firn temperatures and gas close-off depths and ages were determined with $\delta^{18}O_{ice}$ record as a temperature proxy [$\Delta T_s = (1/\alpha)\Delta\delta^{18}O_{ice}$] and an empirical correlation between accumulation rate and temperature (based on the Clausius Clapeyron law) (*6*) as model input. On the basis of these values, thermal (*12*) and gravitational (*11*) enrichments of N_2 for different α scenarios were calculated (first method). Although the accumulation rate increased considerably, from about 0.07 m of ice per year before DO 19 to about 0.21 m of ice per year at the maximum of DO 19 (*6*), the effect on the firn thickness was relatively small because thickening due to an increase of accumulation rate is largely compensated for by the thinning caused by the more rapid sintering associated with higher temperatures. Therefore, calculations of the gravitational enrichment (which was not independently measured) for several scenarios (α = 0.33, 0.50, 0.67 per mil/K) show little change in the gravitational enrichment. A maximum change of +0.05 per mil is found for α = 0.67 per mil/K (+0.03 per mil for α = 0.33 per mil/K), 350 years after the onset of temperature increase. A sensitivity study performed with the f function calculation method (*13*) showed that these small gravitational enrichments have only a minor influence on α (≤0.03 per mil/K).

The $\delta^{15}N$ changes were determined from measurements and modeling (Fig. 2). The best fit was obtained for α = 0.47 ± 0.05 per mil/K, resulting from linear interpolation between the model results for α = 0.45 and 0.50 per mil/K. Additionally, the measured mean $\delta^{15}N$ before the event, 0.47 per mil, is similar to the modeled one of 0.46 per mil (α = 0.45 per mil/K) but different from the values of the other scenarios, which are 0.58 per mil (α = 0.33 per mil/K) and 0.38 per mil (α = 0.67 per mil/K). One uncertainty in this method is the potential change in the size of the convective zone, which is difficult to determine. Estimated present-day values for the Greenland Summit are small, with an upper limit of 5 m (*18*). The good agreement of measured and modeled $\delta^{15}N$ values before the DO 19 event (see above) indicates a similarly small convective zone for the studied period. The results of the second method indicate that no large changes in the convective zone occurred during this event (see below). A change in the convective zone of 5 m would correspond to a temperature change of 1.8 K.

The second method to derive α uses the Δages from the model. The Δages obtained for the start of the DO event 19 can be compared with the measured age differences (see Fig. 1). This method is independent of the convective zone depth, because the change in gas age at bubble close-off is negligible compared with the ice age change, and of uncertainties in the

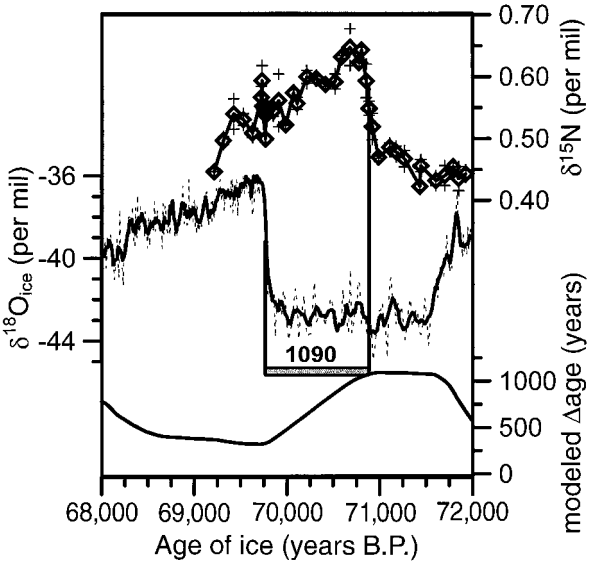

Fig. 1. $\delta^{15}N$ (single values: +; mean values of two parallel samples: ◇) and $\delta^{18}O_{ice}$, versus ice age [according to GRIP SS09 age scale (*17*)]. $\delta^{18}O_{ice}$ is shown in full resolution (dashed line: ~7 cm) and slightly smoothed (solid line: seven-value running mean). Because the gas and the ice signals are caused by the same temperature event (the onset of DO 19), the differences in the ice ages correspond to Δages. Δages from best-fitting model calculations are shown by the bottom curve.

extent of the $\delta^{15}N$ change but depends on the correlation between accumulation rate and temperature. Our $\delta^{15}N$ record (Fig. 3) is shown with curves for different scenarios of Δage and $\delta^{18}O_{ice}$. The best agreement for the rise in $\delta^{18}O_{ice}$ and $\delta^{15}N$ is found for $\alpha = 0.41 \pm 0.07$ per mil/K.

The slight disagreement between the two methods used to calculate α may result from a change in the height of the convective zone. The higher value of the first method requires an increase of the size of the convective zone of about 5 to 6 m with increasing temperature to agree with the lower α value obtained by the second method. This is not consistent with observations, because an increase in temperature is normally accompanied by lowered wind speeds (*19*), which should lead to lower wind pumping and therefore to a shallower convective zone depth. It is more plausible that the accumulation rate–temperature relation may have been different from what we have assumed. The relation we used, derived by fitting a quadratic exponential function to accumulation data and the corresponding $\delta^{18}O_{ice}$ values calibrated with borehole temperatures (*6*), is uncertain because of the large scatter in the reconstructed accumulation rates and might be valid only over the long term and for mean values. A time-dependent relation has been proposed by Kapsner *et al.* (*20*).

The question arises of whether a relation between $\delta^{18}O_{ice}$ and accumulation rate during DO 19 that is consistent with both α derivation methods exists. To investigate this, we applied an exponential relation between $\delta^{18}O_{ice}$ and accumulation rate (*21*) and performed some tests, changing values of the parameters of the exponential relation, considering that (i) the present accumulation rate is correct and (ii) the age of DO 19 remains unchanged. The ice accumulation rate = 0.23 $\times$ exp[0.142 per mil^{-1} $\times$ ($\delta^{18}O_{ice}$ +34.83 per mil)] (meters per year) is consistent with both methods for $\alpha = 0.42 \pm 0.05$ per mil/K. This relation implies a 10% higher accumulation rate at full glacial conditions compared with the one given by Johnsen *et al.* (*6*). The range of the corresponding surface temperature change for the α value of 0.42 per mil/K is 14.3 K to 18.1 K with an best estimate of 16.0 K [this range results mainly from the uncertainty of the gravitational enrichment (~30%) and from the $\delta^{15}N$ measurements (~60%)]. This α is substantially different from the values derived from borehole temperatures ($\alpha = 0.33$ per mil/K), which is, however, not surprising because the borehole temperatures reflect the long-term change from the Last Glacial Maximum (LGM) to the Holocene. One explanation for this difference in α may be a different temperature change in the subtropical moisture region. Recent studies have indicated a tropical sea surface temperature change of about 5 K during the LGM-Holocene transition (*22*), which implies an even larger change in the subtropical moisture source region. During the DO 19, however, the record of atmospheric methane suggests a rather minor temperature change in the tropics and subtropical regions (*23*, *24*). When we compare a 15 K cloud temperature change over Central Greenland for a situation with an approximately constant moisture source temperature as assumed for DO 19 with a situation where the moisture source temperature increases by 5 K during the climate change as we suppose for the LGM-Holocene transition, a simple Rayleigh-type model (*25*) implies an α that is about 10 to 30% higher for the constant moisture source temperature situation. Therefore, the difference in the source temperature change may explain at least part of the difference in α that we observe in comparison with the long-term borehole measured α, which is valid for the LGM-Holocene transition. An additional change in the circulation regime, a change in the distribution of summer and winter snow, or a different change in cloud temperature may also play a role.

A continuous record of $\delta^{15}N$, providing temperature change information and Δages over a whole ice core, would not only give detailed information on the variation of the $\delta^{18}O_{ice}$-temperature relation but would also help to improve ice core time scales. The latter requires firn densification and ice flow modeling.

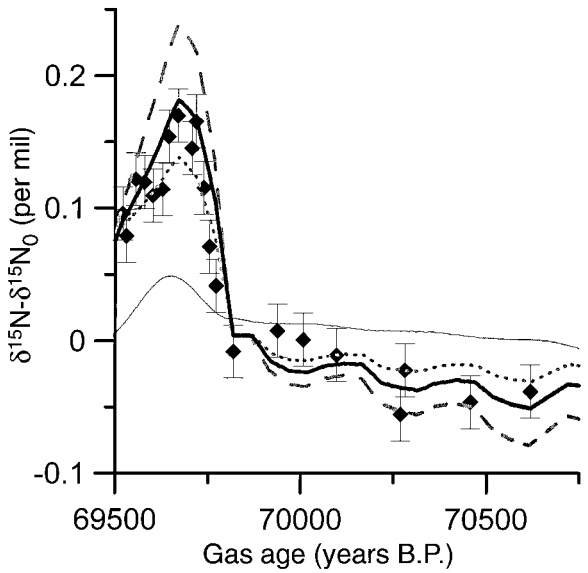

Fig. 2. Variations in $\delta^{15}N$ from measurements (◆) and model calculations (*7*). Three model scenarios are shown for $\alpha = 0.45$ per mil/K (solid black line), $\alpha = 0.33$ per mil/K (gray dashed line), and $\alpha = 0.67$ per mil/K (gray dotted line). For the accumulation-temperature relation of Johnsen *et al*. (*6*), a best fit is found for $\alpha = 0.47 \pm 0.05$ per mil/K. The offset for the measurements, $\delta^{15}N_0$, essentially identical to the gravitational enrichment at the beginning of the DO19 (a slight thermal nonequilibrium, originating from the previous DO event, has an additional influence), is 0.47 per mil. For the model results, it is 0.46 per mil ($\alpha = 0.45$ per mil/K), 0.58 per mil ($\alpha = 0.33$ per mil/K), and 0.38 per mil ($\alpha = 0.67$ per mil/K). Error bars represent the (conservative) laboratory reproducibility of 0.02%. (The deviation of the parallel samples is less than 0.01%.) The thin line corresponds to the change of the gravitational fractionation over time ($\alpha = 0.45$ per mil/K) referenced to $\delta^{15}N_0$.

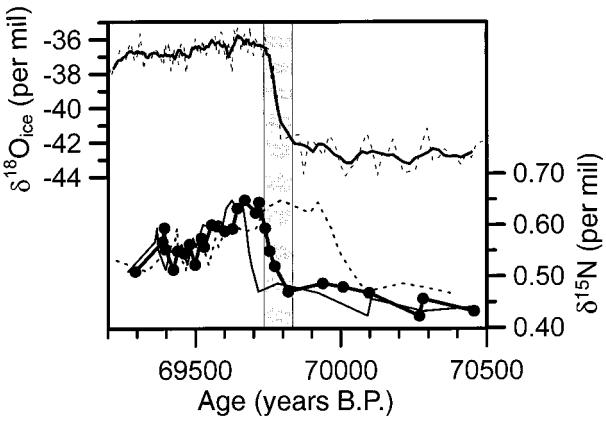

Fig. 3. $\delta^{15}N$ data (gas age) plotted with Δages from model calculations for the accumulation rate of Johnsen *et al*. (*6*). The two extreme cases [$\alpha = 0.33$ per mil/K (thin solid line) and $\alpha = 0.67$ per mil/K (thin dashed line)] and a fit of $\alpha = 0.40$ per mil/K (dots and solid line) are shown in comparison with the $\delta^{18}O_{ice}$ signal at the top (ice age, lines types as in Fig. 1). The shaded area marks the main increase in $\delta^{18}O_{ice}$ at the beginning of DO 19.

References and Notes

1. δ notation: $\delta^{18}O = [(^{18}O/^{16}O)_{sample}/(^{18}O/^{16}O)_{standard} - 1] \times 1000$ per mil.
2. S. J. Johnsen *et al.*, *Nature* **235**, 429 (1972).
3. W. Dansgaard *et al.*, *Science* **218**, 1273 (1982); S. J. Johnsen *et al.*, *Nature* **359**, 311 (1992); P. M. Grootes *et al.*, *Nature* **366**, 552 (1993); J. F. Adkins *et al.*, *Nature* **390**, 154 (1997); L. D. Keigwin *et al.*, *Nature* **371**, 323 (1994); C. D. Charles *et al.*, *Earth Planet. Sci. Lett.* **142**, 19 (1996); R. J. Behl and J. P. Kennett, *Nature* **379**, 243 (1996); H. Schulz, U. von Rad, H. Erlenkeuser, *Nature*

393, 54 (1998); N. Thouveny *et al.*, *Nature* **371**, 503 (1994); E. C. Grimm *et al.*, *Science* **261**, 198 (1993); H. Mommersteeg, thesis, University of Amsterdam (1998).
4. J. Johnsen, W. Dansgaard, J. W. C. White, *Tellus Ser. B* **41**, 452 (1989).
5. K. M. Cuffey *et al.*, *J. Glaciol.* **40**, 341 (1994); K. M. Cuffey *et al.*, *Science* **270**, 455 (1995).
6. S. Johnsen, D. Dahl-Jensen, W. Dansgaard, N. Gundestrup, *Tellus Ser. B* **47**, 624 (1995).
7. J. Schwander *et al.*, *J. Geophys. Res.* **102**, 19483 (1997).
8. J. P. Severinghaus *et al.*, *Nature* **391**, 141 (1998).
9. A. Mariotti, *Nature* **303**, 685 (1983).
10. H. Craig, Y. Horibe, T. Sowers, *Science* **242**, 1675 (1988).
11. J. Schwander, in *The Environmental Record in Glaciers and Ice Sheets*, H. Oeschger and C. C. Langway Jr., Eds. (Wiley, New York, 1989), pp. 53–67.
12. S. Chapman and T. G. Cowling, *The Mathematical Theory of Non-Uniform Gases* (Cambridge Univ. Press, Cambridge, 1970).
13. M. Leuenberger, C. Lang, J. Schwander, *J. Geophys. Res.* **104**, 22163 (1999).
14. V. Boersma-Klein and A. E. De Vries, *Physica* **32**, 717 (1966).
15. We determined $\delta^{15}N$ on gas from samples of the GRIP ice core from depths between 2552 and 2567 m [69,215 to 71,925 years B.P. ice age (*17*), about 68,850 to 71,100 years mean gas age (*7*)]. Seventy-four samples (each about 21 g) from 36 different depth levels were analyzed. The mean resolution for the samples is thus 40 cm or ~75 years ice age (~60 years mean gas age difference). The resolution is higher during the transition to the DO 19, namely ~25 cm (64 years ice age and 15 years mean gas age difference; the gas resolution due to gas mixing by diffusion and close-off process is lower, namely 50 to 100 years). The air was released from the ice with a melt extraction technique. After evacuation, the ice samples underwent a melting-refreezing cycle twice to liberate the enclosed gas from bubbles and clathrates. The gas then passed through a water trap cooled with liquid nitrogen and was frozen at 20 K. After this procedure, less than 0.005% of the gas was left. The samples were then analyzed with a MAT-250 mass spectrometer for several isotope and element ratios. ^{15}N and ^{14}N were measured simultaneously in relation to a standard gas with a reproducibility of 0.02 per mil. Results are given as $\delta^{15}N$, that is, the per mil deviation from the atmospheric isotope ratio, $^{15}N/^{14}N$. The overall uncertainty is less than 0.05 per mil. $\delta^{18}O_{ice}$ measured with the standard CO_2 equilibrium method in Copenhagen and Reykjavik (*17*) shows an uncertainty of 0.05 per mil.
16. H. R. Phillpot and J. W. Zillman, *J. Geophys. Res.* **75**, 4161 (1970).
17. S. Johnsen *et al.*, *J. Geophys. Res.* **102**, 26397 (1997).
18. M. A. Hutterli, R. Röthlisberger, R. C. Bales, *Geophys. Res. Lett.* **26**, 1691 (1999); J. Schwander *et al.*, *J. Geophys. Res.* **98**, 2831 (1993); C. M. Trudinger *et al.*, *J. Geophys. Res.* **102**, 6747 (1997).
19. P. A. Mayewski *et al.*, *J. Geophys. Res.* **102**, 26345 (1997).
20. W. R. Kapsner *et al.*, *Nature* **373**, 52 (1995).
21. D. Dahl-Jensen, S. J. Johnsen, C. U. Hammer, H. B. Clausen, J. Jouzel, in *Ice in the Climate System, NATO ASI Series*, vol. I12 (Springer-Verlag, Berlin, 1993), pp. 517–532; J. Jouzel *et al.*, *Quat. Res.* **31**, 135 (1989).
22. C. Charles, *Nature* **385**, 681 (1997).
23. E. J. Brook, T. Sowers, J. Orchardo, *Science* **273**, 1087 (1996).
24. Because the atmospheric methane is believed to have been primarily related to the tropical and subtropical hydrological cycle [A. Dällenbach *et al.*, in preparation; J. Chappellaz *et al.*, *Nature* **366**, 443 (1993)], a small methane variation at DO 19 [as indicated by the methane record (*23*), but in low resolution] could mean small temperature and precipitation changes in these regions.
25. J. Jouzel *et al.*, *J. Geophys. Res.* **102**, 26471 (1997).
26. This work is a contribution to the Greenland Ice Core Project (GRIP), a European Science Foundation program with eight nations and the European Economic Commission collaborating to drill through the central part of the Greenland Ice Sheet. This special study was financially supported by the Bundesamt für Energie and the Swiss National Science Foundation (including the Swiss Priority Programme Environment) as well as the European Community project MILECLIM (contract ENV4-CT97-0659). We thank T. Stocker for helpful discussion and comments and P. Nyfeler for technical assistance.

19 May 1999; accepted 7 September 1999

Seismic Consequences of Warm Versus Cool Subduction Metamorphism: Examples from Southwest and Northeast Japan

Simon M. Peacock[1]* and Kelin Wang[2]

Warm and cool subduction zones exhibit differences in seismicity, seismic structure, and arc magmatism, which reflect differences in metamorphic reactions occurring in subducting oceanic crust. In southwest Japan, arc volcanism is sparse and intraslab earthquakes extend to 65 kilometers depth; in northeast Japan, arc volcanism is more common and intraslab earthquakes reach 200 kilometers depth. Thermal-petrologic models predict that oceanic crust subducting beneath southwest Japan is 300° to 500°C warmer than beneath northeast Japan, resulting in shallower eclogite transformation and slab dehydration reactions, and possible slab melting.

During subduction, variably hydrated basalts and gabbros of the oceanic crust transform to eclogite, a relatively dense rock consisting primarily of garnet and omphacite (Na-Ca clinopyroxene). The transformation of hydrated metabasalt to eclogite releases substantial amounts of H_2O (*1*) and increases the density of subducting slabs (*2*). Kirby *et al.* (*3*) proposed that dehydration reactions trigger intermediate-depth (50 to 300 km) intraslab earthquakes and suggested that deeper intraslab earthquakes observed in cold subduction zones may reflect kinetic hindrance of eclogite formation. In a given subduction zone, the depth and nature of eclogite formation and slab dehydration reactions depends on the pressure (P)–temperature (T) conditions encountered by the subducting oceanic crust. Temperatures at depth in subduction zones vary because of variations in convergence rate, thermal structure (age and sediment thickness) of the incoming lithosphere, and possibly rates of shear heating (*4*). We present thermal models for the subduction zones of southwest (SW) and northeast (NE) Japan and examine the metamorphic evolution of subducting oceanic crust.

In many subduction zones, detailed seismic investigations reveal the presence of a thin (<10 km thick), low seismic-velocity layer coinciding with the zone of thrust and intermediate-depth earthquakes (*3, 5, 6*). The seismic velocity of eclogite is comparable to mantle peridotite, thus the dipping low seismic-velocity layer is generally interpreted as subducted oceanic crust that has not transformed to eclogite (*3*). Beneath SW Japan, subducted oceanic crust of the Philippine Sea plate is marked by a layer with low P-wave (V_P = 6.6 to 6.9 km s^{-1}) and S-wave (V_S = 3.8 to 3.9 km s^{-1}) velocity which extends to 60 km depth (*7*). Beneath NE Japan, the low-velocity layer, representing subducted oceanic crust of the Pacific plate, persists to 150 km depth and has slightly higher V_P ~ 7.5 km s^{-1} (*5, 8*). Beneath SW Japan, the maximum depth of intraslab earthquakes is ~50 to 65 km (*9*). In NE Japan, intraslab earthquake activity peaks at 125 km depth and extends to 200 km depth (*3*), and deep earthquakes occur down to 670 km depth (*5*).

Abundant Holocene volcanism occurs in NE Japan (Fig. 1) with a well-defined volcanic front located ~100 km above the top of the subducting Pacific plate (*5*). Most NE Japan arc lavas exhibit calc-alkaline geochemistry, which reflects partial melting in the mantle wedge triggered by the infiltration of aqueous fluids derived from the subducting slab (*10*). In SW Japan, Holocene volcanism is relatively sparse. Andesite and dacite erupted at Daisen and Sambe volcanoes in SW Japan (Fig. 1) are geochemically similar to adakites (*11*), which are interpreted to represent partial melts of subducted oceanic crust (*12*).

To understand subduction-zone processes operating at 50 to 200 km depth, we constructed two-dimensional, finite-element heat-transfer models for NE and SW Japan along the profiles

[1]Department of Geology, Arizona State University, Tempe, AZ 85287–1404, USA. [2]Pacific Geoscience Centre, Geological Survey of Canada, Sidney, BC V8L 4B2, Canada.

*To whom correspondence should be addressed. E-mail: peacock@asu.edu

16°C Rapid Temperature Variation in Central Greenland 70,000 Years Ago

C. Lang, M. Leuenberger, J. Schwander and S. Johnsen

Science **286** (5441), 934-937.
DOI: 10.1126/science.286.5441.934